Title	Evaluation of Elastic Properties in C/C Composites by means of FEM Analysis of Fiber Indentation Tests(Mechanics, Strength & Structure Design)
Author(s)	Serizawa, Hisashi; Sato, Shinji; Tsunakawa, Hideo et al.
Citation	Transactions of JWRI. 1997, 26(2), p. 43-48
Version Type	VoR
URL	https://doi.org/10.18910/4402
rights	
Note	

Evaluation of Elastic Properties in C/C Composites by means of FEM Analysis of Fiber Indentation Tests †

Hisashi SERIZAWA*, Shinji SATO**, Hideo TSUNAKAWA*** and Akira KOHYAMA****

Abstract

To investigate the mechanism of energy loss in load - displacement of indenter curve (indentation curve) under fiber indentation test of unidirectionally reinforced C/C composites, the fiber indentation tests were performed and the indentation curve was analyzed by an axis symmetrical finite-element method (FEM) model including a newly designed fiber-matrix interfacial bonding. In this model, only elastic deformations were considered for both fiber and matrix, and the interfacial bonding was assumed to yield not to fracture. From this FEM analysis, a hysteresis loop was obtained in the indentation curve and the interfacial debonding was founded to start from the inside of specimen under the indentation test. And the indentation curve calculated by the FEM analysis was coincide with the experimental results, so compressive Young's modulus of carbon fiber in C/C composite was founded to be predictable from the FEM analysis.

KEY WORDS: (C/C composite) (Carbon fiber) (Indentation test) (Interface) (Finite element method) (Young's modulus) (Transmission electron microscopy) (Graphite)

1. Introduction

Mechanical properties of the interface between fibers and matrices are known to be quite influential in determining properties of fiber reinforced composites. Some previous reports have indicated the effectiveness of controlling fiber-matrix interfaces in improving properties of composite materials [1]. So the effects of surface treatments and coatings on fibers for several composites have been studied [2] and many experiments have been carried out to measure the interfacial mechanical properties by various methods, such as the pull-out test [3], push-out test [4], protrusion test [5] and multiple fracture test [6]. Most of these studies have done by using simple model composites reinforced with a single thick fiber. But practical carbon reinforced carbon (C/C) composites employ a large number of very thin fibers and have many pores and cracks in the matrix [7]. Hence measurement of the mechanical properties of practical C/C composites on the micro scale is very difficult and the micro indentation test is considered to be one of the suitable test methods.

There have been some reports of indentation tests on carbon materials [8], but in these reports maximum load and displacement of the indenter were too large to apply to only one fiber in the practical C/C composites. So, to study the mechanical properties of fiber, matrix and their interfaces in C/C composites, the authors have applied a newly developed ultra micro indentation test machine [9)-11)]. Where, indications of plastic deformation were not observed on specimen surfaces after the indentation test using scanning electron microscopy (SEM), although load - displacement of the indentation curve showed a large hysteresis loop, it was concluded that indicated some energy loss had occurred during test [10]. However this experimental result could not be explained by any models (including the indentation tests of carbon materials) as far as the authors could establish. So, in this study, fiber indentation tests were performed and a new finite-element method (FEM) model was provided for analyzing the deformations of fiber, matrix and their interfaces.

2. Experimental

2.1 Material used and specimen form

Material used was unidirectionally reinforced C/C

† Received on December 5, 1997

* Research Associate, Osaka University
** Professor, Fukushima National College of Technology
*** Research Associate, The University of Tokyo
**** Professor, Kyoto University

Transactions of JWRI is published by Joining and Welding Reseach Institute of Osaka University, Ibaraki, Osaka 567, Japan.

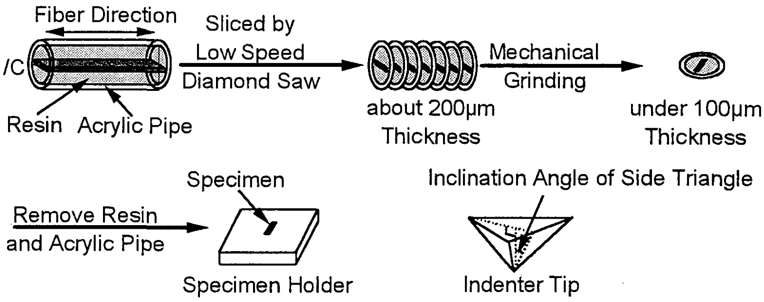

Fig. 1 Schematic flow of specimen preparation and shape of indentation tip

Table 1 Characteristics of fibers used

Diameter (μm)	9.8
Tensile Modulus (GPa)	542
Tensile Strength (GPa)	2.92
Heat Treatment Temperature (K)	2473

composite, heat treated at 1873 K. The carbon fiber used was a mesophase pitch-based fiber and its characteristics are shown in **Table 1**. Matrix precursor was a mixture of green coke and phenolic resin (80/20 in volumetric ratio). And the fiber volume fraction and density of the C/C composite were 45.0 % and 1.69 Mg/m^3, respectively.

The schematic flow of specimen preparation for the fiber indentation test is shown in **Figure 1**. C/C specimens, of size 20^l x 5^w x 1^t mm, were fixed at the center of acrylic pipe by means of resin. The fixed specimen was sliced perpendicular to the fiber direction to about 200 μm thickness with a low speed diamond saw. Then the thickness of the sliced specimen was reduced to 80 μm by mechanical grinding and the pipe and resin were removed in acetone. Finally the size of specimen for fiber indentation test became 5^l x 1^w x 0.08^t mm.

2.2 Fiber indentation test

Fiber indentation tests were carried out by utilizing the dynamic ultra indentation test machine [8]. The specimen was placed on a holder made of SUS and fibers in C/C composites were loaded under a triangular diamond pyramid indenter tip, where maximum loads were 0.2 N. The shape of triangular diamond pyramid indenter tip is shown in Fig. 1. The inclination angle of the side triangle was 68 degrees.

2.3 Structural inspections

Macroscopic structure, including fiber volume fraction, was determined by both optical microscopy and SEM. And microstructural inspections of interfaces were performed with high resolution transmission electron microscopy (TEM : JEOL-4000FX), where the acceleration voltage was 400 kV. Specimens for TEM observation were prepared by dimple grinding and Ar ion milling, and were observed parallel to the fiber direction.

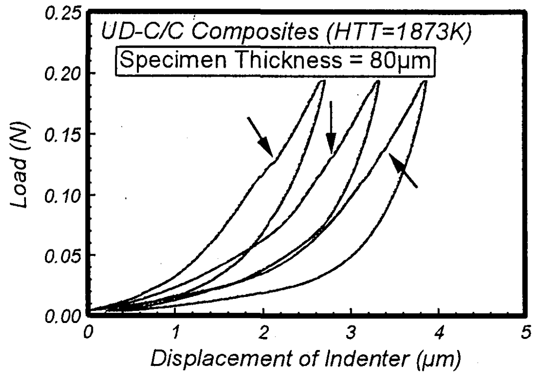

Fig. 2 Indentation curves under fiber indentation test in C/C composites

3. Results of Fiber Indentation Test

Typical examples of indentation curves are shown in **Figure 2**. For all cases, the indentation curves showed large hysteresis loops and come back to the origin. Under indentation tests of glasslike carbon, similar hysteresis loops were reported [8]. However maximum loads and displacements of the indenter were over 10 N and 100 μm, respectively. In addition, cracks were observed at the specimen surface after carbon indentation tests by SEM. But, in the fiber indentation tests, the interfacial debonding and the indentation mark could not be observed at the specimen surface. This suggests that the origin of the hysteresis loops under the fiber indentation tests was different from that under the carbon indentation tests, that is, the loops under the fiber indentation tests were not arising from the essential property of carbon.

Micro steps which can be detected in Fig. 2 and indicated by arrows, are considered to be indications of interfacial debonding. So, for the exact understanding of the indentation curves and the deformations of fiber,

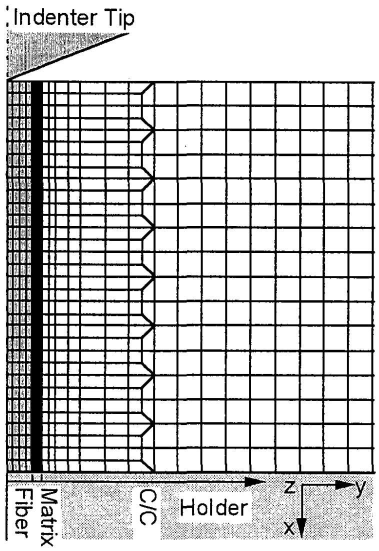

Fig. 3 FEM model of fiber indentation test

matrix and interface in C/C composites under such a test, a new FEM analysis including the interfacial debonding seems to be needed.

4. FEM Model

4.1 Shape of the FEM model

By using an axis symmetrical FEM model shown in **Figure 3**, the deformations of fiber, matrix and interface in C/C composite under fiber indentation test were calculated. For the analysis of practical composites, the correlation between adjacent fibers must be taken into account, but in this study, two dimensional models were used for the first step of the FEM examination including the interfacial debonding. So C/C composites reinforced with only single carbon fiber were used for this calculation, and the matrix phase was assumed to be the carbon. The width of this layer was assumed to be 2 μm, which reflects a fiber volume fraction in specimens for fiber indentation tests correctly (**Figure 4**).

Under the indentation test, the effect of the area of contact between indenter tip and specimen on stress distribution was considered to be very large [10]. For this axis symmetrical FEM model, the shape of the indenter tip was a cone not a triangular pyramid. Therefore, in this analysis, the indenter tip was assumed to be a cone with 145.6 degree apical angle so that the area of contact in the case of the cone was the same as in the case of the triangular pyramid at the same displacement of indenter, shown in **Figure 5**.

4.2 Interfacial bonding between fiber and matrix

Figure 6 shows a typical example of a TEM image of the interface between fiber and matrix. The vertical

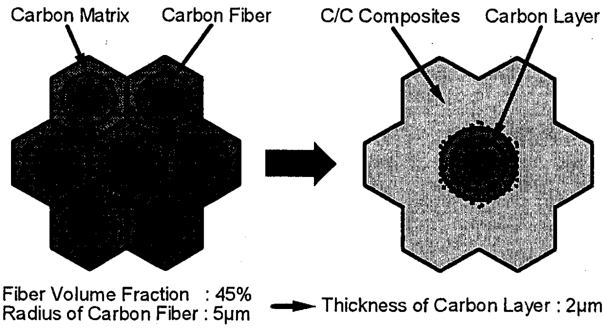

Fig. 4 Thickness of carbon layer around fiber

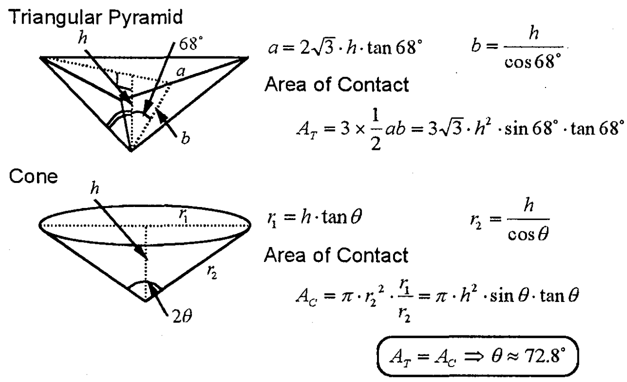

Fig. 5 Shape of indenter tip

direction of this figure is also the fiber direction. From this figure, the thickness of the interface seems to be about 30 nm. The structure of carbon at the interface was observed to be consist of graphite layers parallel to the fiber direction. That is, the c-axis direction of this graphite was parallel to the radial direction of the fiber. For graphite structures, bonding strength in the c-axis direction is very weak because there are van der Waals bonds between graphite layers [7]. So the debonding of the fiber-matrix interface is considered to be as same as the debonding between the graphite layers.

In most previous analyses of micro indentation tests, an extra interphase, arising from the reaction of fiber and matrix, was set up independently [12]. For C/C composites, the extra interphase seems to be the graphite layer. In the present FEM analysis, the graphite layers were assumed to be springs between the nodes of fiber and matrix elements in the FEM model, and debonding was assumed to occur when a length of the spring, that was 30 nm in the beginning of the FEM analysis, changed to 45 nm, indicating that the distances between each graphite layers expand to one and half times. Stiffness of the spring parallel and transverse to the fiber direction were determined to the 50 GPa and 20 GPa, respectively, from the mechanical properties of graphite [13].

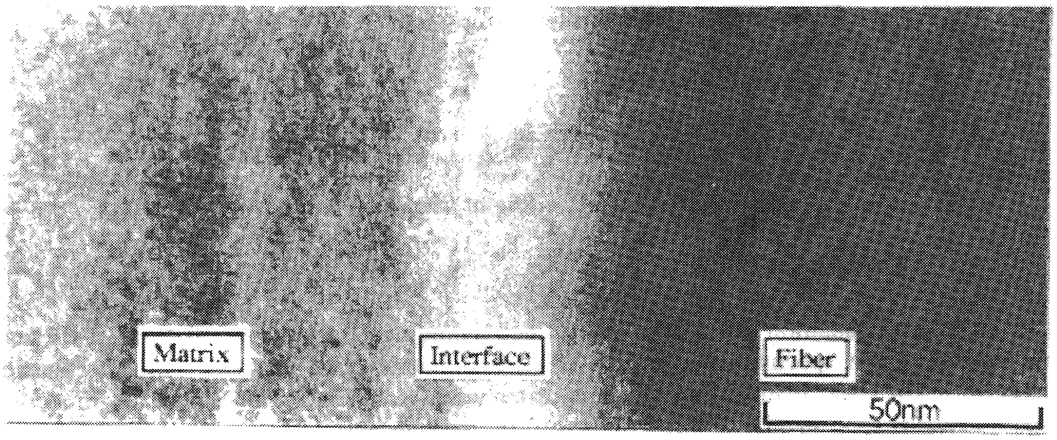

Fig. 6 TEM image at interface between fiber and matrix

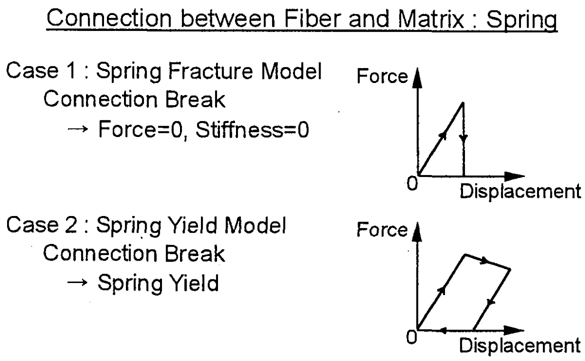

Fig. 7 Condition of debonding at fiber-matrix interface

Two types of stress-transmission mechanism in the spring were proposed as shown in **Figure 7** to explain the debonding at fiber-matrix interfaces. In Fig. 7, case 1 is the usual method of interfacial debonding for FEM analysis under the fiber indentation test. Under the conditions of case 1 in the axis symmetrical FEM model, debonding at one point on the fiber surface seems to be equivalent to a debonding on a circumference. But this model is not considered to exactly express a three dimensional situation of the debonding at the fiber-matrix interface, because in three dimensions debonding at one point on fiber surface seems to be gradually spread around the circumference, including the debonding point. So a second interfacial bonding mechanism was constructed and is shown in case 2 of Fig. 7. Under this condition in case 2, the bonding force of the spring between fiber and matrix was assumed to decrease linearly after the beginning of the interfacial debonding, and this is considered to indicate the gradual spread of the interfacial debonding. Interfacial bonding was thus presumed not to yield to fracture. The slope of the bonding force during unloading in the fiber indentation test was assumed to be the same as that during loading, because the bonding between fiber and matrix was considered to be supported by the residual bonding interface which has the same stiffness in both loading and unloading.

Table 2 Conditions of FEM model

Analysis Model	Axis Symmetrical FEM Model
Specimen Size :	Radius 2500 μm, Thikness 80 μm
Radius of Fiber :	5 μm
Indenter Tip :	Cone with 145.6° of the Apical Angle
Thickness of Carbon Layer	:2 μm (from Fiber Volume Fraction)
Elastic Properties of Each Element	
Fiber :	E_{xx}: 80GPa ν_{xy}:0.16 G_{xy}:10GPa E_{yy}: 8.9GPa ν_{yz}:0.30 G_{yz}:20GPa E_{zz}: 8.9GPa ν_{zx}:0.16 G_{zx}:10GPa Density 2.08 Mg/m^3
Carbon Layer :	E: 8.9GPa ν: 0.30 Density 1.70 Mg/m^3
C/C :	E_{xx}: 40GPa ν_{xy}:0.20 G_{xy}:8.9GPa E_{yy}: 8.9GPa ν_{yz}:0.30 G_{yz}:15GPa E_{zz}: 8.9GPa ν_{zx}:0.20 G_{zx}:8.9GPa Density 1.68 Mg/m^3

4.3 Condition of FEM model

After the fiber indentation test, the interfacial debonding and the indentation mark could not be observed at the specimen surface by SEM. So, in this FEM analysis, only the elastic deformations of fiber, matrix and C/C composites were considered. The origin of the large hysteresis loop in Fig. 2 was assumed to be an energy loss caused by the fiber-matrix interfacial debonding. The specimen holder and the indenter tip were presumed to be rigid. The conditions of FEM analysis are as shown in **Table 2**. The Young's moduli of C/C composites were determined from the measured values [14], except for the longitudinal Young's modulus of unidirectional C/C composites. The radial Young's

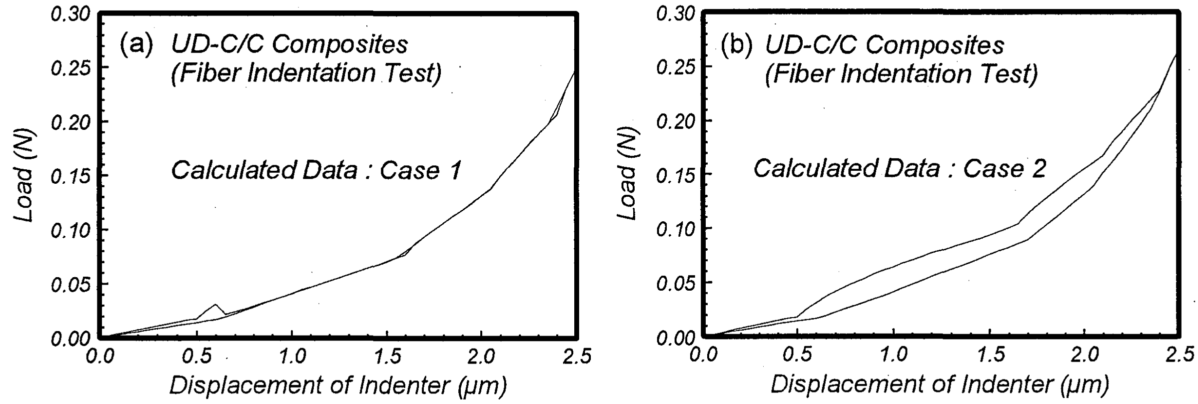

Fig. 8: Indentation curves calculated from FEM model with the interfacial bonding of case 1 (a) and case 2 (b)

modulus of fiber and the isotropic Young's moduli of matrix were assumed to be same as the transverse Young's modulus of unidirectional C/C composites. And the Poisson's Ratio and the shear modulus were determined from the previous researches [15] except for ν_{xy} and ν_{zx} of fiber, which were decided in reference to the Poisson's Ratio of composite and fiber.

On the other hand, the carbon fiber was considered to be the main recipient of the compressive stress at the fiber direction under the fiber indentation test, and the compressive Young's modulus of fiber has been reported to be one quarter of the tensile Young's modulus [16]. And the longitudinal Young's modulus of fiber is known to be strain dependent. So the longitudinal Young's modulus of carbon fiber was assumed to be one quarter of the calculated value from the longitudinal Young's modulus of unidirectional C/C composites [14] according to the simple law of mixture, and the longitudinal Young's modulus of C/C composites was determined from this.

5. Results of FEM Analysis

In this FEM analysis, only the displacement of the indenter can be controlled. So the FEM analyses with the two kinds of interfacial bonding, i.e. case 1 and 2, were conducted in loading from 0 to 2.5 μm displacement of indenter and in unloading from 2.5 to 0 μm displacement. The indentation curves calculated from the FEM model with the interfacial bonding of cases 1 and 2 are shown in **Figure 8** (a) and (b), respectively. In Fig. 8 (a), the load was largely decreased over 0.6 μm displacement of indenter, and the interfacial debonding started after the 0.6 μm displacement. But the large decrease of load was not detected in the experimental results. On the other hand, for the FEM model with the interfacial bonding of case 2, the load was continuously increased although the interfacial debonding began after the 0.6 μm displacement. The indentation curve for case 2 showed the hysteresis loop similar to the experimental results. So the FEM model with the interfacial bonding of case 2 is considered to be suitable for the analysis of the fiber indentation test of C/C composites.

In this FEM analysis for case 2, the start point of the interfacial debonding was the inside rather than the surface of the specimen. Interfacial debonding started at the interface, at 5 μm depth from the upper side of the specimen surface. And the area of interfacial debonding gradually expanded into the lower side of the specimen surface with increasing displacement of the indenter, although interfacial debonding at both the upper and lower sides of specimen surface did not occur at the 2.5 μm displacement of the indenter. This result from the FEM analysis was in good agreement with the result by the SEM observation of the specimen surface after the fiber indentation test. Furthermore, in this FEM analysis for case 2, the maximum value of load at the 2.5 μm displacement of indenter was close to the experimental results. Therefore the compressive Young's modulus of carbon fiber in C/C composites was founded to be predictable from the FEM analysis with the new interfacial bonding mechanism.

6. Conclusions

To investigate the mechanism of the energy loss indicated by the indentation curve from fiber indentation tests of C/C composites, the tests were performed and the indentation curve was analyzed by an axis symmetrical FEM model including a newly designed fiber-matrix interfacial bonding mechanism. The conclusions can be summarized as follows.

(1) From the FEM analysis, the hysteresis loop was obtained in the indentation curve and interfacial debonding was founded to start from the inside of specimen during fiber indentation test.

(2) The indentation curve calculated by this FEM analysis coincided with the experimental results, so the compressive Young's modulus of carbon fiber in C/C composites was founded to be predictable from this FEM analysis.

Acknowledgments

The authors would like to express their sincere appreciations to Dr. E. Tsushima and Mr. J. Takayasu (TONEN Co.) for providing materials and to Mr. M. Fukunaga (Nippon MARC Co., Ltd.) for fruitful discussion.

References

1) M. Leparoux, L. Vandenbulcke, S. Goujard, C. Robin-Brosse and J. M. Domergue : Mechanical Behavior of 2D-SiC/BN/SiC Processed by ICVI, Proceedings Tenth International Conference on Composite Materials, Canada, 1995, Vol. IV, 633-640.
2) D. H. Grande, J. F. Mandell and K. C. C. Hong : Fiber-Matrix Bond Strength Studies of Glass, Ceramic, and Metal Matrix Composites, Journal of Materials Science, Vol. 23 (1988), 311-328.
3) P. Lawrence : Some Theoretical Considerations of Fibre Pull-Out from an Elastic Matrix, Journal of Materials Science, Vol. 7 (1972), 1-6.
4) D. B. Marshall : An Indentation Method for Measuring Matrix-Fiber Frictional Stresses in Ceramic Composites, Journal of the American Ceramic Society, Vol. 67 (1984), C-259-C-260.
5) Y. Kagawa and K. Honda : A Protrusion Method for Measuring Fiber/Matrix Sliding Frictional Stresses in Ceramic Matrix Composites, Ceramic Engineering and Science Proceedings, Vol. 12 (1991), 1127-1138.
6) D. B. Marshall and A. G. Evans : Failure Mechanisms in Ceramic-Fiber/Ceramic-Matrix Composites, Journal of the American Ceramic Society, Vol. 68 (1985), 225-231.
7) C. R. Thomas : Essentials of Carbon-Carbon Composites, The Royal Society of Chemistry, 1993.
8) M. Sakai, H. Hanyu, and M. Inagaki : Indentation-Induced Contact Deformation and Damage of Glasslike Carbon, Journal of the American Ceramic Society, Vol. 78 (1995), 1006-1012.
9) K. Hamada, S. Sato, H. Tsunakawa and A. Kohyama : Interfacial Microstructure and Mechanical Properties of C/C Composites, Proceedings Tenth International Conference on Composite Materials, Canada, 1995, Vol. VI, 423-430.
10) H. Serizawa, A. Kohyama, K. Watanabe, T. Kishi and S. Sato : Elastic FEM Analysis of Fiber Push-Out Test for C/C Composites, Materials Transactions, JIM, Vol. 37 (1996), No. 3, 409-413.
11) K. Watanabe, A. Kohyama, S. Sato, H. Serizawa, H. Tsunakawa, K. Hamada and T. Kishi, : Evaluation of Interfacial Shear Strength of C/C Composites by means of Micro-Indentation Test, Materials Transactions, JIM, Vol. 37 (1996), No. 5, 1161-1165.
12) H. C. Tsai, A. M. Arocho and L. W. Gause : Prediction of Fiber-Matrix Interphase Properties and their Influence on Interface Stress, Displacement and Fracture Toughness of Composite Material, Materials Science and Engineering, A126 (1990), 295-304.
13) B. T. Kelly : Physics of Graphite, Applied Science Publishers, London and New Jersey, 1981.
14) H. Serizawa, A. Kohyama and S. Sato : Effect of Heat Treatment Temperature on Young's Modulus and Internal Friction of C/C Composites, Proceedings of the Ninth International Conference on Composite Materials, Spain, 1993, Vol. 2, 524-531.
15) P. R. Goggin : The Elastic Constants of Carbon-Fibre Composites, Journal of Materials Science, Vol. 8 (1973), 233-244.
16) A. H. Shinohara, T. Sato, F. Saito, T. Tomioka and Y. Arai : A Novel Method for Measuring Direct Compressive Properties of Carbon Fibers Using A Micro-Mechanical Compression Tester, Journal of Materials Science, Vol. 28 (1993), 6611-6616.